

# The Ovalisation of Steel Circular Hollow Sections under Bending

Amer M. Ibrahim<sup>1</sup>, Manahel Sh. Khalaf<sup>\*,2</sup>

<sup>1</sup> Professor, <sup>2</sup> M.Sc. Student, Department of Civil Engineering, Engineering College, University of Daiyla

manahelshahath@gmail.com

## Abstract

This paper investigates the ovalisation behavior of the Steel Circular Hollow Sections (CHSs) when subjected to bending moment. The experimental program included testing of ten specimens in four groups in order to examine the influence of changing the diameter, thickness, length and the presence of openings on the ovalisation phenomenon of these specimens.

The experimental results showed that the ovalisation of the specimen cross-section appears clearly when the diameter to thickness ratio (D/t) is ranging from 17 to 50, while the ovalisation of the specimens that have D/t ratio greater than 50 is very little or unclear because the instability of these specimens are controlled by the local buckling. In addition, the change of the specimen length and the presence of openings didn't cause the cross-section ovalisation.

**Keywords:** Circular Hollow Sections, Ovalisation, Bending, Diameter to thickness ratio, Local buckling and Cross-section behavior.

**Paper History:** Received: (19/9/2016), Accepted: (12/12/2016)

## Introduction

At the present time, the Steel Circular Hollow Sections (CHSs) become more popular in the construction applications and thus working to attracting a lot of research efforts in order to determine the structural behavior of these sections.

These sections offer good strength to weight ratio, ductility and compression and torsion resistance properties because of the uniform distributed of the cross section materials about the polar axis that leads to the good performance of these sections and thus increase the scope for using in the structural applications [1, 2, 3, 4].

In this paper, the ovalisation behavior of steel circular hollow specimens under bending is considered because the circular tubes when subjected to bending moment will happen deformation in their cross section, which leads to the occurrence of the phenomenon of the ovalisation for circular sections. The increase

in bending moment will cause gradual growth of the ovalisation phenomenon and thus lead to a gradual decrease in the bending rigidity of the specimens. When the value of the ovalisation reach to the critical value, the circular hollow specimens will be subjected to the local buckling [5, 6, 7].

There are many investigation and theoretical predications about study of collapse behavior for CHS. Lee, et al. [8] presented a study about the stability of circular hollow sections under bending. This study showed that increasing of cyclic bending in the tube caused gradual growth for accumulation ovalisation in circular hollow sections that lead to occur the buckling. Elchalakani, et al. [9] showed that the ovalisation phase has constant load with increasing the bending rotation and this stage is larger for specimens with large diameter to thickness ratio.

## Experimental Work

### Specimen preparation

The experimental program included a total of ten tests on circular hollow specimens with different diameter, thickness and length as shown in Table 1.

Table 1 Dimensions of test specimens.

Sp. No.	D/mm	t/mm	D/t	L/mm	Openings No.
BT1	101.6	3	33.87	1500	Without
BT2	101.6	2	50.8	1500	Without
BT3	101.6	6	16.93	1500	Without
BT4	101.6	3	33.87	1500	1 opening at mid-span
BT5	101.6	3	33.87	1500	2 openings at loading points
BT6	101.6	3	33.87	1500	3 openings at mid-span and loading points
BT7	101.6	3	33.87	2000	Without
BT8	101.6	3	33.87	1000	Without
BT9	219	3	73	1500	Without
BT10	76.2	3	25.4	1500	Without



**Figure 1:** Circular collars of the experimental study.

These collars used for the following:

- Supporting the vertical load.
- Prevent the concentration of stress at a certain point by through ensuring the radial distribution of the applied load.
- Support the compression part of the specimen effectively and thus will prevent the development of the local buckling at the loading points.
- Restrict the radial displacement at the loading points as a result of the high rigidity and stiffness of this collars.
- Reduce the imperfections and deviations that appear in the top part of the specimen's cross section when subjected to the longitudinal compression during the tests.
- Prevent the sudden failure of the specimens when they reach to the ultimate load.

**Material properties**

This study used the tensile test in order to determine the properties of the steel specimens. This study is prepared the tensile specimens according to ASTM (A370) specifications as shown in Figure 2 and were tested by using the tensile test machine to determine the properties of these specimens such as the yield stress of specimen  $F_y$  and the ultimate stress  $F_u$  as shown in Table 2.

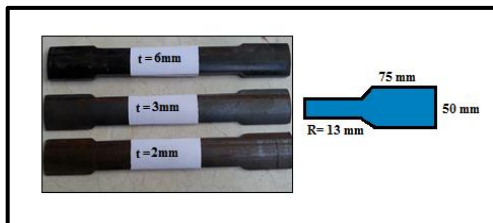


**Figure 2:** Tensile specimen dimensions

Table 2 Tensile test results of the specimens.

Sp. No.	t /mm	$F_y$ (MPa)	$F_u$ (MPa)
BT1	3	290	370
BT2	2	360	430
BT3	6	285	440
BT4	3	290	370
BT5	3	290	370
BT6	3	290	370
BT7	3	290	370
BT8	3	290	370
BT9	3	290	370
BT10	3	290	370

**Test setup**

The setup of four-point bending test is shown in Figure 3, the specimen placed between two supports and the vertical load was applied in the center of the specimen by using the hydraulic jack, which was associated with the load cell and attached to the spreader beam. After that the applied load was transferred equally to the specimen at two loading points through the spreader beam.



**Figure 3:** Setup of four-point bending test.

For measurement the cross-section ovalisation during the specimens loading, this study was used two dial gauges, one of them was placed in the front side and the other in the back side of the cross-section at the center of specimen as shown in the Figure 3.

**Results and Discussion:**

**Effect of the D/t ratio on the specimen ovalisation**

The cross-section behavior of the specimens BT1, BT2 and BT3 during the loading process is shown in Figures 4 to 7. From Figure 4, it can be noted that the cross-section of the specimen BT1 didn't show any response in the elastic zone but when access to yield load equal to 45 kN, the back side of the cross-section began to subject to compression

deformation accompanied by the curvature of specimen.

The cross-section of the specimen BT2 showed its response from beginning of loading as shown in Figure 5, this cross-section began to change gradually by exposure the front side to tension deformation and the back side to compression deformation which means the specimen ovalisation.

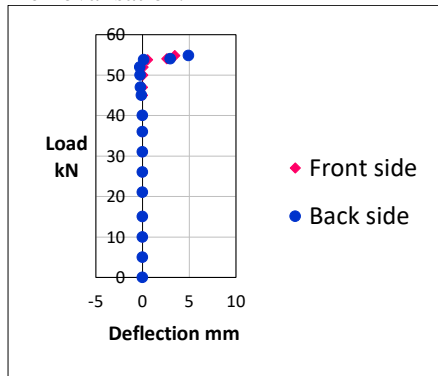


Figure 4: Cross-section behavior of the specimen BT1

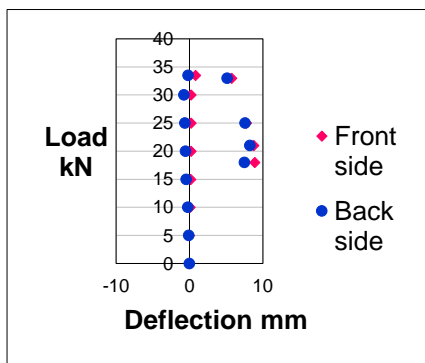


Figure 5: Cross-section behavior of the specimen BT2

While the cross-section of the specimen BT3 began its response to applied loads at load= 10 kN as shown in Figure 6 through the tension deformation in front side and the compression deformation in back side. These deformations were in continuous increasing with the increase of applied loads on this specimen up to yield load= 85 kN.

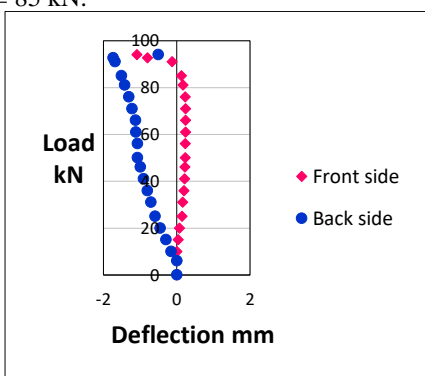
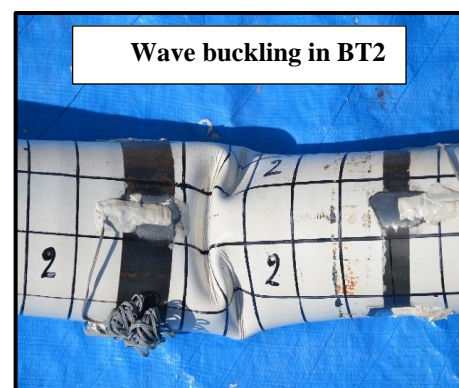


Figure 6: Cross-section behavior of the specimen BT3

After the yield load, the stresses redistribution occurred due to the strain hardening capacity which led to subject the front side of cross-sections of specimen BT1 to tension deformation. While the front side of specimen BT3 became exposure to compression deformation.

Increasing the applied loads on the specimens BT1, BT2 and BT3 led to increasing the cross-section deformation and its transformation to oval shape accompanied by decrease the bending stiffness of these specimens, and this case continued up to ultimate load equal to 54.8, 33.5 and 99.6 kN respectively.

After that, it was noticed that the ovalisation phenomenon for these specimens converted to localization deformation by the occurrence of a kink in the top part of specimen BT1 and formation of wave buckling in compression part of the specimen BT2 as shown in Figure 7. In this stage, both sides of the cross-section for the specimen BT1 and BT2 behave in the same way by exposure them to tension deformation. The gradual growth in the cross-section for the specimen BT3 led to increase the curvature of the top and bottom surface. After that, the negative stiffness controlled these specimens and make them unstable and finally caused the structural collapse.



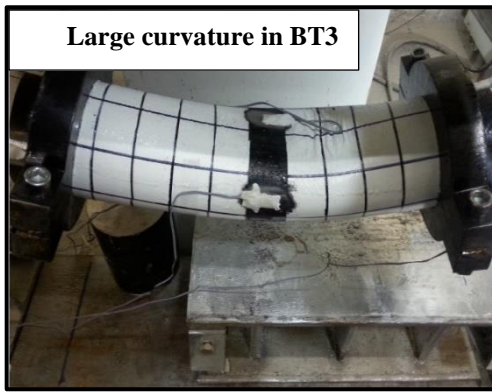


**Figure 7:** Cross-section ovalisation of the specimens BT1, BT2 and BT3

The gradual change in the cross-section of the specimens BT9 occurred from the loading beginning with very small response through the tension deformation in front side and the compression deformation in back side as shown in Figure 8. While both sides of specimen BT10 began their response by the tension deformation as shown in Figure 9, this case continued up to the yield load.

After this load, the stresses redistribution occurred and caused the exposure of front side of the specimen BT10 to compression deformation while the tension deformation in back side continued to increase with the applied loads. But when the specimen BT9 arrived to yield load= 160 kN, it was observed a reduction in the front side deformation.

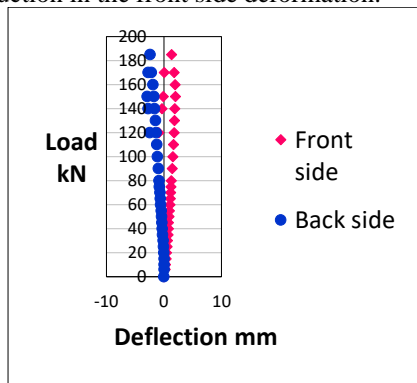


**Figure 8:** Cross-section behavior of the specimen BT9

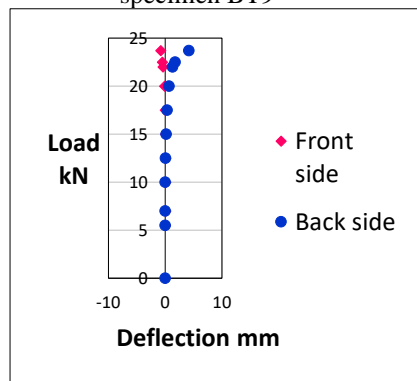


**Figure 9:** Cross-section behavior of the specimen BT10

This change in the cross-section caused a decrease in the specimen bending stiffness therefore the specimens ovalisation converted to the localization phenomenon by the fold composition in compression part of the specimen BT9 at the right loading point accompanied by transformation the tension deformation in front side to compression deformation. While the localization of the specimen BT10 began by the kink formation in compression part, eventually this led to structural failure for these specimens as shown in Figure 10.

The Figure 11 shows the change of the cross-section diameter for the specimens BT1, BT2, BT3, BT9 and BT10 with the change of D/t ratio at the ultimate load. The specimens BT1 and BT10 attained an increase in the diameter of its cross-section by 8.27% and 4.46% respectively compared with the initial diameter. The specimen BT2 showed a very little increase in its diameter equaled to 0.6% compared with the initial diameter as a result of the small thickness, which led to occurrence of wave buckling in the top part and reduce the cross-section ovalisation. While the cross-section diameter of the specimen BT3 and BT9 showed a reduction by 1.56% and 0.49% respectively compared with the initial diameter, this is due to the large thickness of the specimen BT3 which increase its resistance to cross-section deformation and because the large diameter of the specimen BT9 which caused the local buckling.

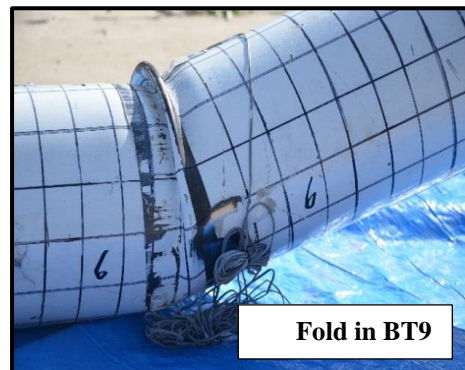


**Figure 10:** Cross-section ovalisation of the specimens BT9 and BT10



From this, we observe that when the D/t ratio for the specimens is less than 16.93 and greater than 50.8, the ovalisation of the cross-section is very little or unclear because the instability of the specimens that have D/t ratio greater than 50.8 are controlled by the local buckling. But when the D/t ratio of the specimens is ranging (17-50), an increase occurs in the diameter of the cross-section which lead to a clear ovalisation for the specimens as a result of the instability of these specimens are controlled by the ovalisation.

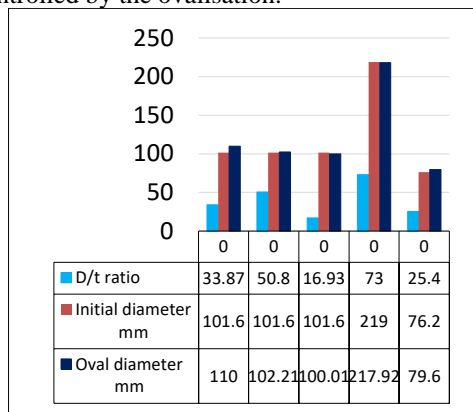


Figure 11: Change of cross-section diameter of the specimens BT1, BT2, BT3, BT9 and BT10 at ultimate load

**Effect of the openings on the specimen ovalisation**

The cross-section behavior of the specimens BT4, BT5 and BT6 during the loading processes is shown in Figures 12 to 15. From the beginning of the specimens loading, the cross-section started to ovalisation through the gradual change in the section diameter which occurred as a result of exposure the front side to tension deformation and the back side to compression deformation in the specimen BT4 as shown in Figure 12 and by the compression deformation in front side and the tension deformation in back side in the specimen BT5 as shown in Figure 13.

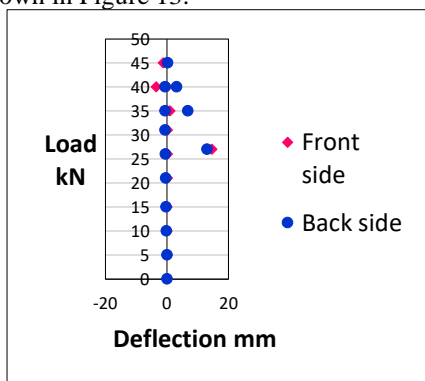


Figure 12: Cross-section behavior of the specimen BT4

While both sides of the specimen BT6 showed compression deformation but the front side gave more response than the back side with increasing the applied loads as shown in Figure

14 as a result of the presence of openings in the front side. Increasing the applied loads on the specimens BT4, BT5 and BT6 led to the gradual growth of the cross-section ovalisation and caused a high reduction in bending stiffness, this case continued up to ultimate load= 45, 44 and 47 kN respectively.

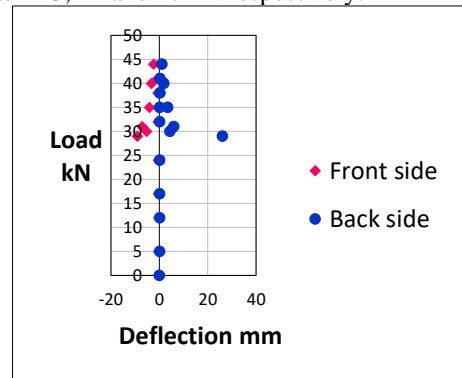


Figure 13: Cross-section behavior of the specimen BT5

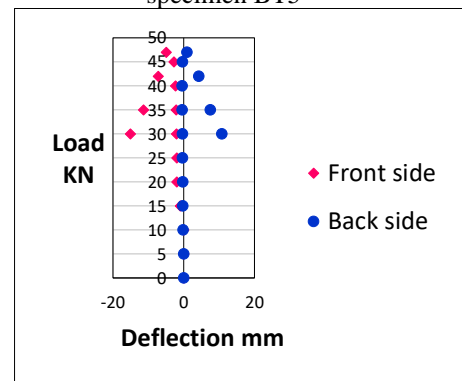
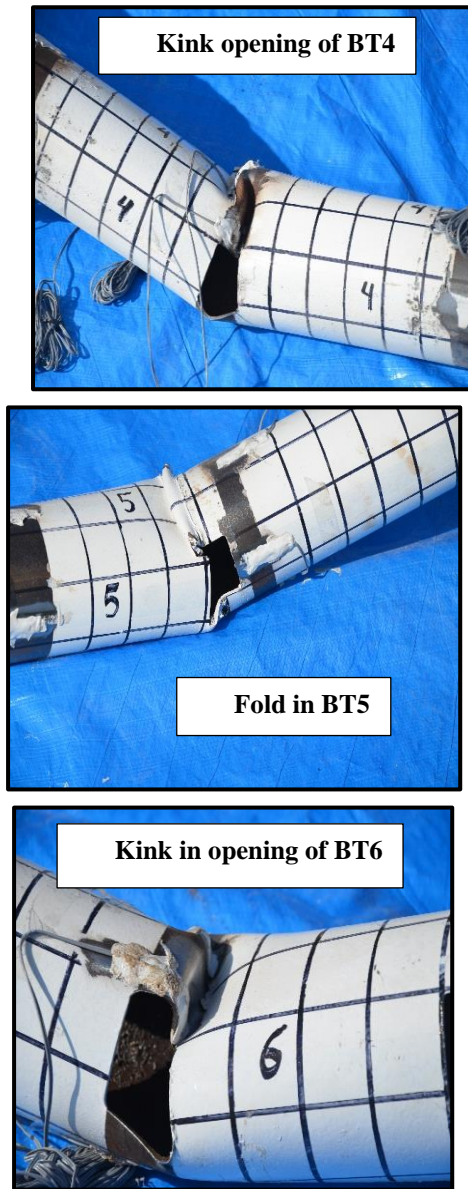


Figure 14: Cross-section behavior of the specimen BT6

At the ultimate load, it was noticed that the front side of the specimen BT4 began to tension deformation and this is due to the high plastification that occurred in top surface of the opening, which led to transformation the ovalisation phenomenon to localization deformation that characterized by the formation of the kink in that surface accompanied by exposure the both sides to tension deformation.

But when specimen BT5 reached the ultimate load= 44 kN, it was noticed that a high increase occurred in this response, after that a fold formed in the top surface at the left loading point within the pure bending region. This fold led to localization phenomenon and caused the structural collapse for this specimen as shown in Figure 15.



**Figure 15:** Cross-section ovalisation of the specimens BT4, BT5 and BT6

When the specimen BT6 reached to the ultimate load, it was observed that the back side gave the tension deformation in the front side remained in continuous increase with the applied loads. And thus led to kink formation in top surface of the central opening due to the negative stiffness which caused the structural collapse for this specimen.

The change of the cross-section for the specimens BT1, BT4, BT5 and BT6 with the same D/t ratio at the ultimate load is shown in Figure 16. From this, we note that the cross-section of the specimens BT4, BT5 and BT6 showed a decrease by 0.94%, 1.23% and 4% respectively compared with the initial diameter.

This is due to the presence of openings in the front side of the specimens cross-section that subjected to buckling and caused deformation

to the cross-section and lack of clarity the ovalisation phenomenon.

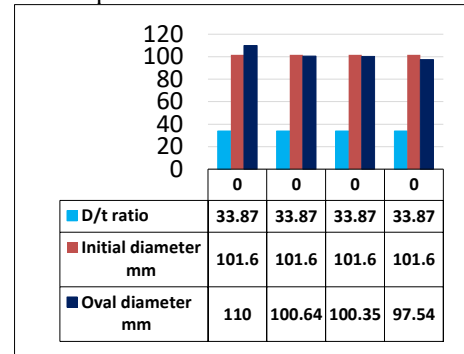


**Figure 16:** Change of cross-section diameter of the specimens BT1, BT4, BT5 and BT6 at ultimate load

#### *Effect of the L/D ratio on the specimen ovalisation*

The cross-section of the specimens BT7 and BT8 began to gradually change from the beginning of loading. Initially, the front side of the specimen BT7 showed a little response which is the compression deformation, later it is exposure to small tension deformation, and the back side of this specimen showed increasing compression deformation with increase the applied loads as shown in Figure 17.

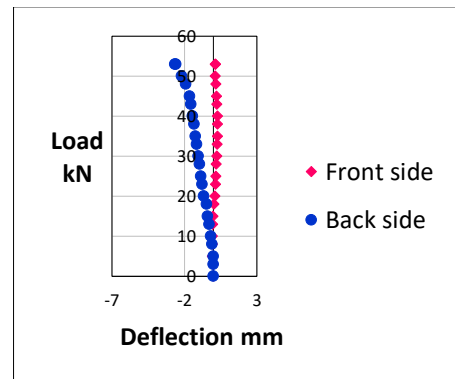


**Figure 17:** Cross-section behavior of the specimen BT7

While the both sides of the specimen BT8 showed the compression deformation which led to the specimen ovalisation through the gradual change that occurred in the cross-section diameter as shown in Figure 18. The cross-section change caused a decrease in the bending stiffness and led to transformation the ovalisation phenomenon to localization that characterized by the formation of kink in the top part of the specimen BT7 and formation of fold beside the right ring in the compression part of the specimen BT8. After that, the gradual growth of the localization phenomenon led to the structural failure for these specimens as shown in Figure 19.

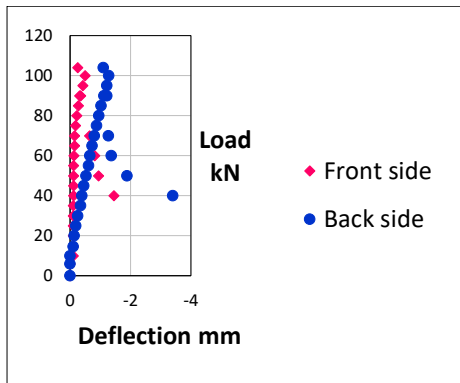


**Figure 18:** Cross-section behavior of the specimen BT8

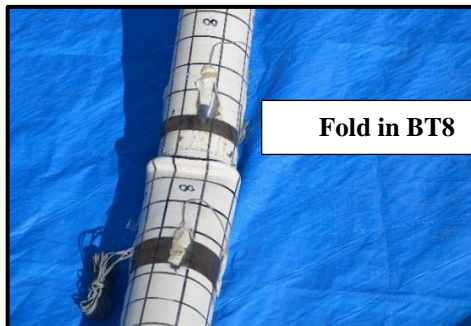


**Figure 19:** Cross-section ovalisation of the specimens BT7 and BT8.  
 Figure 20 gives the change of the cross-section diameter with the L/D ratio for the specimens BT1, BT7 and BT8 at the ultimate load. The specimens BT7 and BT8 showed decrease in their cross-section diameter by 2.45% and 1.33% respectively compared with the initial diameter. From this, we note that the cross-section ovalisation is not depend on the change of the specimen length.

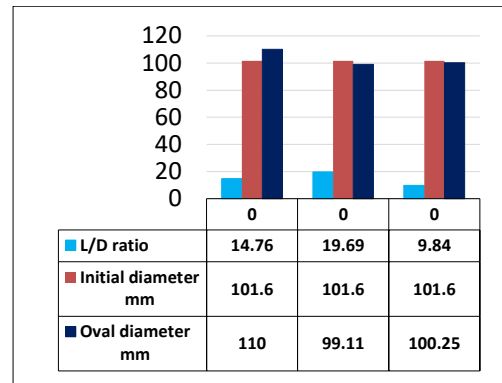


**Figure 20:** Change of cross-section diameter of the specimens BT1, BT7 and BT8 at ultimate load

### Conclusion

This paper has offered the experimental results on steel circular hollow sections. A total of ten specimens were tested with different diameter, thickness, length and number of openings in order to study the ovalisation behavior of their cross-section.

The experimental results showed that the following:

- The ovalisation of cross-section was very little or unclear when the D/t ratio for the specimens is less than 16.93 and greater than 50.8, because the instability of the specimens that have D/t ratio greater than 50.8 are controlled by the local buckling.
- When the D/t ratio of the specimens is ranging (17-50), an increase occurred in the cross-section diameter and led to a clear ovalisation for the specimens.
- Changing the length of the specimen and the presence of openings didn't cause the cross-section ovalisation.

### Acknowledgment

This work was supported by Diyala University, Civil Engineering Department, which is gratefully acknowledged.

**References:**

[1]. Chavan, V. B., Nimbalkar, V. N., and Jasiwal, A. P. Economic evaluation of open and hollow structural sections in industrial trusses. *International Journal of Innovative Research in Science, Engineering and Technology*, 3(2), (2014), 9554-9565.

[2]. Hoshikuma, J. I., and Priestley, M. J. N. Flexural behavior of circular hollow columns with a single layer of reinforcement under seismic loading. *SSRP*, 13, (2000).

[3]. Agarwal, D. S., and Chhatwani, A. C. The economic and structural analysis of hollow structural sections. *International Journal on Recent and Innovation Trends in Computing and Communication*, 3(2), (2015), 57-62.

[4]. Wardenier, J., Packer, J. A., Zhao, X. L., and Van der vege, G. J. Hollow sections in structural applications. Rotterdam, The Netherlands: Bouwen met staal, (2002).

[5]. S. Ueda. Moment-rotation relationship considering flattening of pipe due to pipe whip loading, *Nuclear Engineering and Design* 85, (1985), 251-259.

[6]. G. Kiyamaz. Strength and stability criteria for thin-walled stainless steel circular hollow section members under bending, *Thin-Walled structures* 43, (2005), 1534-1549.

[7]. Elchalakani, M., Zhao, X. L., and Grzebieta, R. H. Bending tests to determine slenderness limits for cold-formed circular hollow sections. *Journal of Constructional Steel Research*, 58(11): 1407-1430.

[8]. Lee, K. L., Pan, W. F., and Kuo, J. N. The influence of the diameter-to-thickness ratio on the stability of circular tubes under cyclic bending. *International Journal of Solids and Structures*, 38(14), (2001), 2401-2413.

[9]. Elchalakani, M., Zhao, X. L., and Grzebieta, R. H. Plastic slenderness limits for cold-formed circular hollow sections. *Australian Journal of Structural Engineering*, 3(3), (2002), 127-141.